Int. J. Heat Mass Transfer. Vol. 17, pp. 1383–1390. Pergamon Press 1974. Printed in Great Britain

CONVECTION FROM PIPE WITH HARMONIC INTERNAL HEAT GENERATION

KAMAL-ELDIN HASSAN*
Faculty of Engineering, Cairo University, Egypt

and

MOUNIR M. HILAL† and GALAL M. ZAKI
Reactors Department, Atomic Energy Establishment, Egypt

(*Received* 21 *September* 1973 *and in revised form* 12 *February* 1974)

Abstract—The dynamic behavior of tubular heating elements with harmonic internal heat generation is studied both analytically and experimentally. The analysis is by the "frequency response" method. Its results are given in terms of the more usual "engineering" criteria. The experimental technique used is described briefly; its results agree with those of the analysis.

NOMENCLATURE

$A, B,$ constants of integration;
$c,$ specific heat [J/kg.K];
$D,$ outside diameter of annulus [m];
$\bar{D},$ function defined by equation (25);
$d_o,$ inner diameter of annulus [m];
$\bar{F},$ function defined by equation (23);
$\bar{G},$ function defined by equation (24);
$\bar{H},$ transfer function;
$h,$ heat-transfer coefficient [W/m^2.K];
$I,$ modified Bessel function of first kind;
$i,$ $\sqrt{(-1)}$, imaginary unit;
$K,$ modified Bessel function of second kind;
$k,$ thermal conductivity [W/m.K];
$L,$ tube length [m];
$N,$ dimensionless parameter defined in equation (8);
$N_{Nu},$ $h(D-d_o)/k_f$, Nusselt number [dimensionless];
$\bar{N}_{p,s},$ function defined by equation (21);
$N_{Re},$ $v(D-d_o)\rho_f/\mu_f$, Reynolds number [dimensionless];
$P,$ power generated per unit volume [W/m^3];
$Q,$ total power [W];
$q(s),$ $\sqrt{(s/N_{Fo})}$;
$R,$ r/r_o, dimensionless radius;
$r,$ radius in test section [m];
$s,$ Laplace's variable;
$T,$ τ/τ_a, dimensionless time;
$t,$ temperature [K];
$v,$ fluid velocity in annulus [m/s];
$X,$ x/L, dimensionless distance;
$x,$ distance measured along test section from coolant inlet [m];
$\alpha,$ thermal diffusivity [m^2/s];
$\theta,$ reduced temperature, defined by equation (7) [dimensionless];
$\rho,$ density [kg/m^3];
$\tau,$ time [s];
$\psi,$ time lag [dimensionless];
$\Omega,$ $\omega\tau_a$;
$\omega,$ angular frequency [rad/s].

Subscript

$a,$ amplitude;
$c,$ cylinder;
$f,$ fluid;
$i,$ inner surface of cylinder;
$in,$ inlet section of annulus;
$m,$ mean;
$o,$ outer surface of cylinder;
0, zero order of modified Bessel function;
1, at $R = 1$, or first order of modified Bessel function.

Superscript

$-,$ Laplace transform of function.

*Now, Visiting Professor, School of Mechanical Engineering, Georgia Institute of Technology, Atlanta, Ga. 30332, U.S.A.

†Now, Associate Professor, Mechanical Engineering Department, Faculty of Engineering, Cairo University, Egypt.

INTRODUCTION

THE STUDY of the dynamic behavior of heating elements with internal heat generation is important in the control of heat exchangers with internal heat sources, particularly nuclear reactors. This importance merited a considerable amount or research work. Exact solutions for the transient cases are given by Arpaci and Clark [1], and by Feretic and Hilal [2]. Feretic and Sultan [3] studied the case of a cylindrical element in which heat is generated randomly with time, but distributed according to a sine function along the element. Their theoretical investigation gives the pertinent amplitude–frequency characteristics, and the standard deviation of temperature.

On the other hand, solutions for temperature transients were obtained by Thorpe [4], and by Solbert and Bakstad [5] by numerical methods.

The present work is a study of the case of a tube in the material of which heat is internally generated uniformly in space, but sinusoidally with time. The established-state temperature amplitude and phase-shift are determined analytically as "frequency response". The well-defined conditions made it possible to compare the analytic results with experimental ones. In the experimental study, a stainless steel tube is heated by a d.c. current that varies sinusoidally with time, and cooled at its outside surface by a steady-flow of water. Good agreement was found between analysis and experiment.

ANALYSIS

The mathematical model for this analysis is a hollow cylinder with internal heat generation. Heat is generated uniformly in the solid part of the cylinder following a harmonic time function. The cylinder is cooled at its outside surface by a fluid flowing steadily in an annular space, and the following conditions are assumed.

(a) Thermal conduction in the axial direction is negligibly small, i.e. $t_c = t_c(r, \tau)$. Variations of t_c with axial distance result from variations in adjacent fluid temperature.

(b) The outer surface of the annulus is perfectly insulated; the cooling fluid exchanges heat with the cylinder only.

(c) The fluid temperature t_f is taken as uniform at any cross-section of the annulus, i.e. $t_f = t_f(x, \tau)$.

(d) The heat-transfer coefficient h between the outer surface of the cylinder and the fluid is constant, independent of both position and time.

(e) The hollow cylinder is insulated at its inner surface.

(f) Establihsed periodic conditions are attained.

(g) All physical properties of both solid and fluid are constants.

Mathematical formulation

The temperature distribution in the solid of the cylinder is governed by the general equation of conduction in one direction; in the present case it has the following form

$$\frac{\partial^2 t_c}{\partial r^2} + \frac{1}{r}\frac{\partial t_c}{\partial r} + \frac{P_a}{k_c}\sin\omega\tau = \frac{1}{\alpha_c}\frac{\partial t_c}{\partial \tau}. \tag{1}$$

In this equation P_a is the constant amplitude of the power input to a unit volume of the cylinder solid, k_c and α_c are the thermal conductivity and diffusivity of the cylinder material, and ω the angular frequency.

The heat convected to the fluid is governed by the following relation

$$\frac{4hd_o}{\rho_f c_f (D^2 - d_o^2)}[t_c(r_o, \tau) - t_f] = \frac{\mathrm{d}t_f}{\mathrm{d}\tau} = \frac{\partial t_f}{\partial \tau} + v\frac{\partial t_f}{\partial x}. \tag{2}$$

Boundary conditions. The boundary conditions for the problem, as formulated above, are

1. An expression of the assumption (e) above, viz.

$$\frac{\partial t_c(r_i, \tau)}{\partial r} = 0. \tag{3}$$

2. Heat transfer at cylinder outer surface gives

$$-k_c\frac{\partial t_c(r_o, \tau)}{\partial r} = h[t_c(r_o, \tau) - t_f(x, \tau)]. \tag{4}$$

3. The fluid enters the annular passage at $x = 0$ at a known constant temperature $t_{f,in}$ i.e.

$$t_f(0, \tau) = t_{f,in}. \tag{5}$$

4. Under the established periodic conditions assumed in (f) above, the angular frequency of the temperature fluctuations in both solid and fluid is ω, the same as that of power.

Dimensionless form. The problem could be set in dimensionless form by defining the following quantities. For the independent variables

$$R = r/r_o, \qquad X = x/L, \qquad T = \tau/\tau_o \tag{6}$$

in the last expression, τ_o is a reference period.

The temperatures, the dependent variables, are reduced to dimensionless form by referring their rise above the fluid inlet temperature to an arbitrary temperature amplitude t_a, hence

$$\theta = (t - t_{f,in})/t_a. \tag{7}$$

According to the above definitions, the reduced temperatures in the cylinder solid and in the fluid are, respectively

$$\theta_c = \theta_c(R, T) \quad \text{and} \quad \theta_f = \theta_f(X, T).$$

The following dimensionless parameters are also defined.

$$\left.\begin{aligned} N_{Fo} &= \alpha_c \tau_o / r_o^2 \quad \text{Fourier number,} \\ N_P &= P_a r_o^2 / k_c t_a, \\ N_{Bi} &= h r_o / k_c \quad \text{Biot number,} \\ N_h &= 4 h d_o \tau_o / \rho_f c_f (D^2 - d_o^2), \\ N_v &= v \tau_o / L, \\ \text{and} \quad \Omega &= \omega \tau_o. \end{aligned}\right\} \tag{8}$$

With these dimensionless quantities defined, the differential equations and boundary conditions, equations (1)–(5) become, respectively:

$$\frac{\partial^2 \theta_c}{\partial R^2} + \frac{1}{R}\frac{\partial \theta_c}{\partial R} + N_P \sin \Omega T = \frac{1}{N_{Fo}}\frac{\partial \theta_c}{\partial T} \tag{9}$$

$$N_h[\theta_c(1, T) - \theta_f] = \frac{\partial \theta_f}{\partial T} + N_v \frac{\partial \theta_f}{\partial X} \tag{10}$$

$$\frac{\partial \theta_c(R_i, T)}{\partial R} = 0 \tag{11}$$

$$\frac{\partial \theta_c(1, T)}{\partial R} = -N_{Bi}[\theta_c(1, T) - \theta_f] \tag{12}$$

$$\theta_f(0, T) = 0. \tag{13}$$

Laplace transformation

Transformation in the usual manner, and substitution into equations (9)–(13) give, respectively

$$\frac{\partial^2 \bar{\theta}}{\partial R^2} + \frac{1}{R}\frac{\partial \bar{\theta}_c}{\partial R} - \frac{s}{N_{Fo}}\bar{\theta}_c = -\frac{\Omega N_P}{s^2 + \Omega^2} \tag{14}$$

$$N_h[\bar{\theta}_c(1, s) - \bar{\theta}_f] = s\bar{\theta}_f + N_v \frac{\partial \bar{\theta}_f}{\partial X} \tag{15}$$

$$\frac{\partial \bar{\theta}_c(R_i, s)}{\partial R} = 0 \tag{16}$$

$$\frac{\partial \bar{\theta}_c(1, s)}{\partial R} = -N_{Bi}[\bar{\theta}_c(1, s) - \bar{\theta}_f] \tag{17}$$

$$\bar{\theta}_f(0, s) = 0. \tag{18}$$

Equation (14) is an inhomogeneous modified Bessel's differential equation of zeroth order; its solution is given by

$$\bar{\theta}_c = AI_o(\bar{q}R) + BK_o(\bar{q}R) + \frac{\bar{N}_{P,s}}{q^2} \tag{19}$$

where

$$\bar{q} = \bar{q}(s) = \sqrt{(s/N_{Fo})} \tag{20}$$

and

$$\bar{N}_{P,s} = \Omega N_P/(s^2 + \Omega^2). \tag{21}$$

The constants A and B could be related through equation (16) and, hence, determined from equation (17). The presence of the local transformed fluid temperature $\bar{\theta}_f$ in the latter equation, makes both of the constants A and B functions of this temperature.

Substitution of the values of A and B thus obtained into equation (19) gives [6]

$$\bar{\theta}_c = \bar{G} \,.\, \bar{N}_{P,s} + \bar{F} \,.\, \bar{\theta}_f. \tag{22}$$

In this relation, the functions $\bar{F}$ and $\bar{G}$ are given by

$$\bar{F} = \bar{F}(r, s) = \frac{N_{Bi}}{\bar{D}(s)} \times [K_1(\bar{q}R_i) \,.\, I_o(\bar{q}R) + I_1(\bar{q}R_i) \,.\, K_o(\bar{q}R)] \tag{23}$$

$$\bar{G} = \bar{G}(R, s) = (1 - \bar{F})/\bar{q}^2. \tag{24}$$

The function $\bar{D}(s)$ in equation (23) is given by

$$\bar{D}(s) = N_{Bi}[K_1(\bar{q}R_i) \,.\, I_o(\bar{q}) + I_1(\bar{q}R_i) \,.\, K_o(\bar{q})] + \bar{q}[K_1(\bar{q}R_i) \,.\, I_1(\bar{q}) - I_1(\bar{q}R_i) \,.\, K_1(\bar{q})]. \tag{25}$$

The appearance of the first order modified Bessel functions I_1 and K_1 in the above expressions is by virtue of the recurrence formulae and the differentials of equations (16) and (17).

As mentioned earlier in connection with the integration constants A and B, the solid temperature at a given cross-section as expressed by equation (22) is a function of the fluid temperature in the same cross-section. The Laplace transform of the latter could be determined in the following manner:

At the cylinder surface, the value of $\bar{\theta}_{c,1} = \bar{\theta}_c(1, s)$ is evaluated from equation (22) as

$$\bar{\theta}_{c,1} = \bar{N}_{P,s}\bar{G}_1 + \bar{F}_1\bar{\theta}_f.$$

In this relation the subscript "1" denotes the value of the function at $R = 1$, the cylinder surface. Substituting for $\theta_{c,1}$ from the above expression into equation (15), and rearranging terms, gives

$$N_v \frac{\partial \bar{\theta}_f}{\partial X} = N_h \bar{G}_1 \bar{N}_{P,s} - (s + N_h - N_h \bar{F}_1)\bar{\theta}_f. \tag{26}$$

Equation (26) is a linear "ordinary" differential equation in $\bar{\theta}_f$ with all the quantities involved independent of the distance X. Using the boundary condition of equation (18), the solution of equation (26) is given by

$$\theta_f = \frac{N_h \bar{N}_{P,s} \bar{G}_1}{s + N_h - N_h \bar{F}_1}\left\{1 - \exp\left[-\frac{s + N_h - N_h \bar{F}_1}{N_v} X\right]\right\}. \tag{27}$$

This equation gives the Laplace transform of the fluid temperature along the cylinder. Substituted into equation (22), it gives the transformed temperature in the cylinder material.

Solution

The transformed solution of the problem is given by equations (22) and (27). A final solution could be obtained by the inverse transformation of these expressions. With appropriate "initial conditions", this

solution would be general, i.e. would give the transient as well as the established-state conditions. In the present case, however, the objective is to find the established-state solution; it could be obtained from equations (22) and (27) in the manner given below without the tediousness of obtaining their inverse transformation.

The established-state solution has the following form, for both the fluid and solid domains [7]

$$\theta = \theta_a \sin(\Omega T - \psi). \tag{28}$$

The temperature amplitudes and phase-shifts, represented by θ_a and ψ in the above equation could be determined by the "frequency response" method [7] from the appropriate transfer functions.

A transfer function $\bar{H}$ is the ratio between the Laplace transforms of the dependent and driving functions. Consequently, the transfer functions for both the fluid and solid are determined from equations (27) and (22), respectively, as

$$\bar{H}_f(X,s) = \frac{\bar{\theta}_f}{\bar{N}_{P,s}} = \frac{N_h \bar{G}_1}{s + N_h(1-\bar{F}_1)} \times \left\{1 - \exp\left[-\frac{s+N_h(1-\bar{F}_1)}{N_v} X\right]\right\} \tag{29}$$

$$\bar{H}_c(R,s) = \frac{\bar{\theta}_c}{\bar{N}_{P,s}} = \bar{G} + \bar{F}.\bar{H}_f. \tag{30}$$

In the "frequency response" method, the amplitude of the dependent function could be obtained simply by multiplying the amplitude of the excitation function by the modulus, or absolute value, of the corresponding transfer function in which the Laplace transform variable s is replaced by $i\Omega$. In the present case, therefore,

$$\theta_{f,a} = N_P |\bar{H}_f(X, i\Omega)| \tag{31}$$

$$\theta_{c,a} = N_P |\bar{H}_c(R, i\Omega)|. \tag{32}$$

The same method gives the phase-shift, or time-lag, as the argument of the transfer function with $i\Omega$ replacing s, therefore

$$\psi_f = \arg \bar{H}_f(X, i\Omega) \tag{33}$$

$$\psi_c = \arg \bar{H}_c(R, i\Omega). \tag{34}$$

In the evaluation of the amplitudes and phase-shifts given by equations (31)–(34), it should be noted that the variable $\bar{q}(s)$ defined by equation (20) is replaced by

$$\bar{q}(i\Omega) = \sqrt{(i\Omega/N_{Fo})}. \tag{35}$$

The resulting modified Bessel functions with imaginary arguments resulting from equations (23) and (25) are then replaced by the appropriate Kelvin (or Thomson) functions using pertinent relations [8]. This substitution results in very complicated functions. However, the calculations were carried out by digital computer, and the computation of numerical values were made through appropriate subroutines.

ANALYTIC RESULTS

Numerical values were computed from equations (31)–(34) for the experimental conditions described later. The following values were, therefore, used in evaluating the parameters of equations (8): $d_0 = 10$ mm, $d_i = 7$ mm, $L = 930$ mm, $k_c = 13{\cdot}8$ W/mK, $\alpha_c = 3{\cdot}6 \times 10^{-6}$ m^2/s.

The reference period τ_o and temperature amplitude t_a were arbitrarily taken as 1 s and 1 K, respectively.

Further, to give the computed results more practical value, the fluid velocity v and the heat-transfer coefficient h are represented through the annulus ratio D/d_o and the Reynolds number N_{Re} in the parameters of equations (8). In particular, the heat-transfer coefficient is calculated from the following relation [9]

$$N_{Nu} = 0{\cdot}038 N_{Re}^{0{\cdot}8} N_{Pr}^{1/3} (D/d_o)^{0{\cdot}15}. \tag{36}$$

Samples of the results obtained are shown in Figs. 1–5. Figure 1 gives the distribution of the temperature amplitude at various cylinder cross-sections. The temperature amplitude θ_a is presented in this and other figures through the "temperature gain", θ_a/N_P. It could be seen that the amplitude is small where cooling is effective. Thus, at a given cross-section the maximum amplitude is at the inner insulated surface of the cylinder and decreases to its least value at the water-cooled outside surface. For a given radius, the amplitude increases with the distance from the fluid inlet, as the cooling effect decreases with the temperature rise of the coolant.

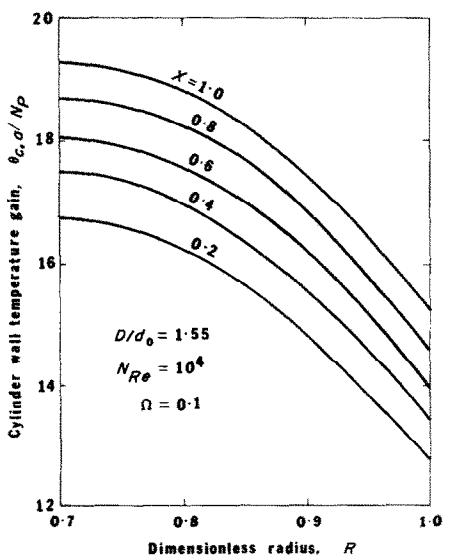

FIG. 1. Distribution of temperature amplitude at various cross-sections of cylinder.

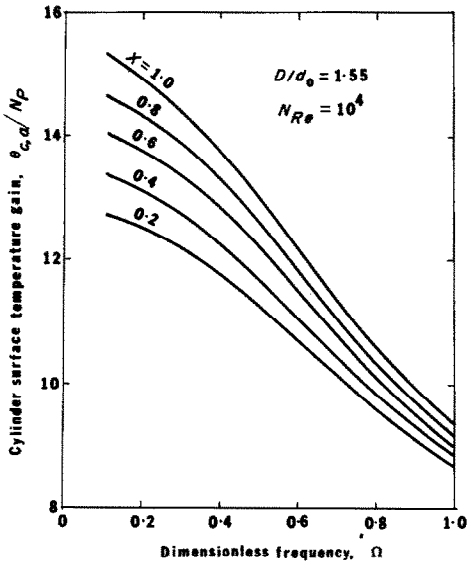

FIG. 2. Variation of temperature amplitude with frequency on the inside surface of cylinder.

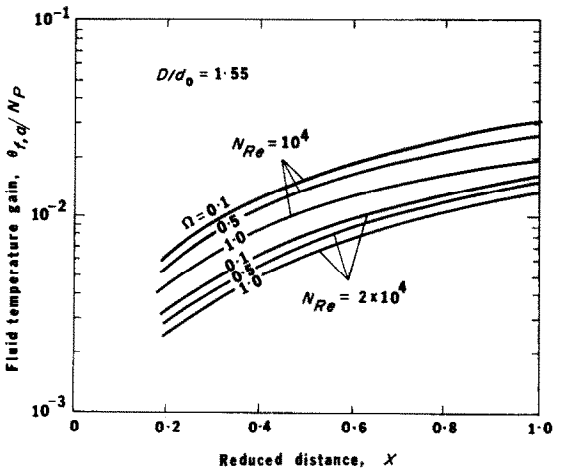

FIG. 3. Temperature amplitude of coolant along annular conduit.

The effect of frequency is shown in Fig. 2. The temperature amplitude at any point on the cylinder surface decreases as the frequency increases. This is a well-known phenomenon, and is due to the cylinder heat capacity that attenuates high frequencies more effectively than low ones.

Figure 3 gives the variation of the fluid temperature amplitude along the annular conduit with frequency, and with Reynolds number. The trends are the same as for the cylinder surface. The fluid temperature amplitude increases with the distance X along the annulus; indeed, because the fluid enters the annulus

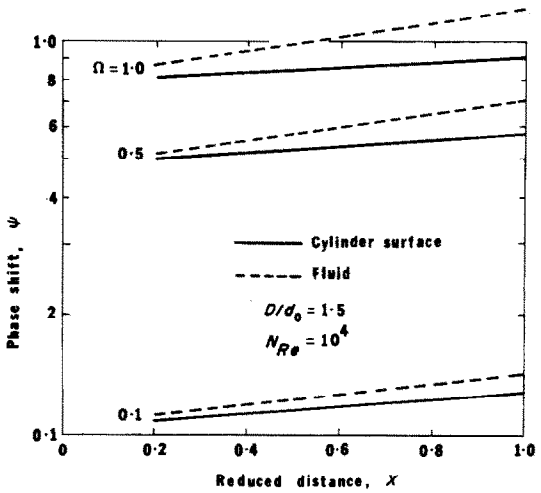

FIG. 4. Phase-shift of temperature at cylinder surface and of coolant along annular conduit.

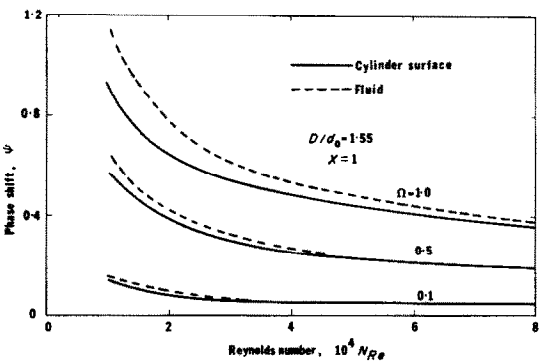

FIG. 5. Effect of Reynolds number on phase-shift at exit ($X = 1$).

at a steady temperature. This amplitude increases with the decrease of frequency. Further, a comparison of the two sets of curves in Fig. 3 shows that the fluid temperature amplitude decreases as the Reynolds number increases. The reason is that, all other conditions being the same, the fluid heat capacity rate increases with Reynolds number.

The effects of the various parameters on the phase-shift, or time-lag are shown in Figs. 4 and 5. For both the cylinder surface (or anywhere in the solid) and the fluid, the time lag increases with the distance X along the annular conduit, and with the decrease of frequency as shown in Fig. 4. The figure also shows a phase shift between the cylinder surface temperature and that of the fluid at any cross-section, with the fluid temperature lagging. This trend is naturally expected, and this time-lag increases with the distance X.

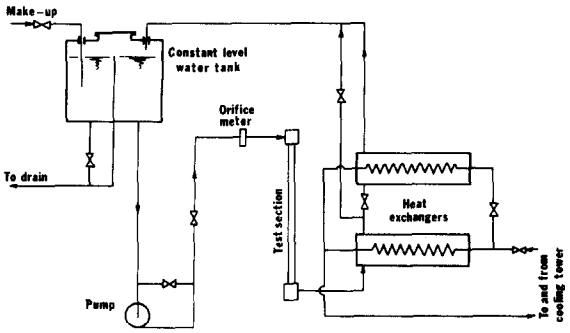

FIG. 6. Primary circuit of experimental loop.

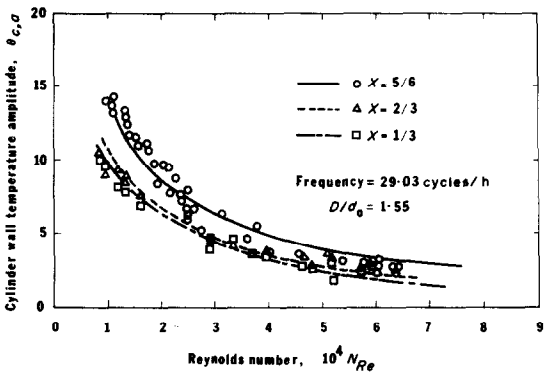

FIG. 7. Variation of temperature amplitude along wall surface with Reynolds number.

Figure 5 shows the effect of Reynolds number on the phase-shift of both the cylinder surface and fluid temperatures at the fluid exit. The time-lag decreases with the better cooling of increased Reynolds number and, as before, with the decrease in frequency.

EXPERIMENTS

The mathematical solution given in the previous part is carried out under the simplifying assumptions enumerated therein. To estimate the effect of these assumptions, experiments were carried out on an apparatus built to represent the mathematical model practically.

The apparatus is shown diagrammatically in Fig. 6. The cylinder was modelled by a vertical stainless steel tube of the dimensions mentioned earlier. Care was taken in the design and manufacture of the end headers to ensure concentricity of the cylinder in the annulus, freedom of motion due to relative thermal expansion, tightness, ample electric insulation, and, as much as possible, a swirl-free flow of the coolant in the annulus. To exclude the possibility of generating joulean heat, distilled water was used as coolant. Heated distilled water was cooled in two heat exchangers by ordinary water in a secondary circuit which comprises a cooling tower.

The d.c. power is supplied to the "cylinder" from a motor-generator set. Rectified a.c. current is fed through a rotating rheostat of uniform speed to supply field current of sinusoidal form to the d.c. generator. This fluctuating current results in sinusoidal voltage for the d.c. power supplied to the test section.

The cooling water flow was measured with an error of about one per cent by a sharp edged orifice. Copper–constantan thermocouples made from 0·25 mm wires were used to measure the water inlet and exit temperatures, and the surface temperature of the cylinder at five cross-sections. The error involved in these measurements, including the dynamic error, is also about one per cent.

The power and frequency were determined from strip chart recordings. The errors involved were estimated to be within 2·3 and 0·8 per cent respectively.

EXPERIMENTAL RESULTS

Experiments were carried out under various conditions, and readings were taken after attaining established conditions. Representative results are shown in Figs. 7–11. These figures give the experimental results in various dot shapes, together with the corresponding analytic results in line forms.

There are some differences between analysis and experiments in Figs. 7–9 at Reynolds numbers higher than about 4×10^4. These are for the temperature amplitudes at $X = 5/6$ on the cylinder surface. These differences are probably due to the inevitable change in flow pattern just before and in the exit header, a change that considerably decreases the local heat transfer coefficient and, hence, enhances the temperature amplitude. This change in flow pattern becomes more pronounced at high Reynolds numbers.

Generally speaking, however, all the figures show good agreement between theory and experiment, and support the trends previously explained in conjunction with Figs. 2–5.

Of particular interest are Figs. 9 and 11; they show the effect of the annulus ratio on the temperature amplitude at the cylinder surface and fluid exit, respectively. For a given Reynolds number, an increase in the annulus ratio is accompanied by a decrease in the heat transfer coefficient h and, consequently, in the cooling effect of the water. This results in an increase in the cylinder surface temperature amplitude as shown in Fig. 9. On the other hand, an increase in the annulus ratio at a given Reynolds number means an increase in the mass flow rate of water. This, together with the increase in thermal resistance between the fluid and cylinder surface, results in a decrease in the water temperature amplitude as indicated in Fig. 11.

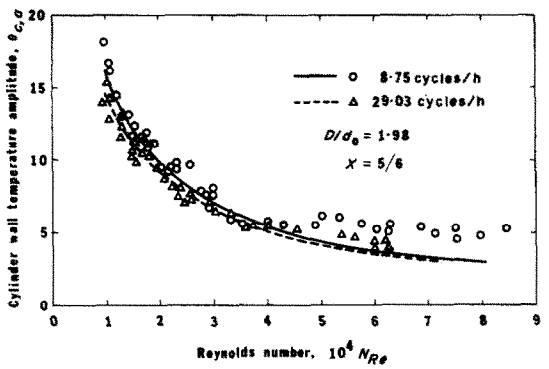

FIG. 8. Variation of cylinder surface temperature amplitude with Reynolds number and frequency.

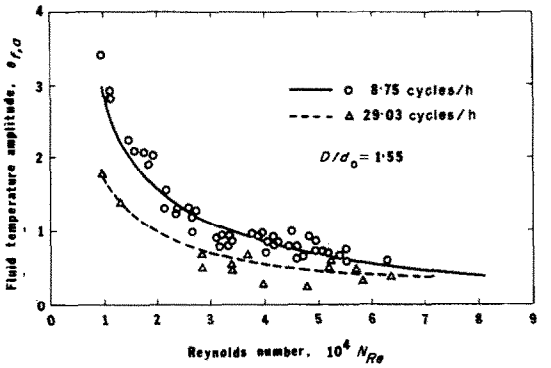

FIG. 10. Variation of fluid temperature amplitude with Reynolds number and frequency.

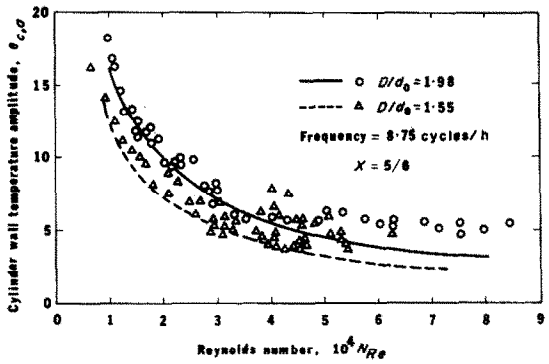

FIG. 9. Variation of cylinder surface temperature amplitude with Reynolds number and annulus ratio.

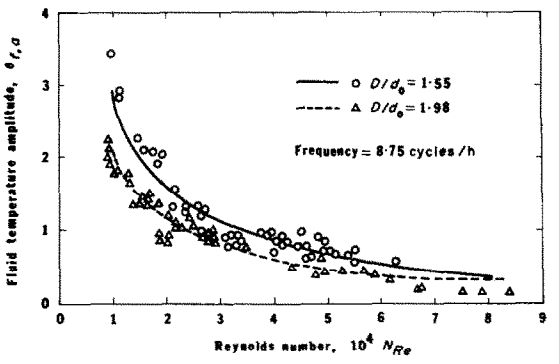

FIG. 11. Variation of fluid temperature amplitude with Reynolds number and annulus ratio.

CONCLUSIONS

Analysis is carried out to predict the dynamic behavior of a cylinder internally heated according to a harmonic function, and its steady-flow coolant. Experiments were carried out on a test section similar to the mathematical model. Close agreement was found between experimental and analytic results.

Acknowledgement—This work was possible through the support and facilities of the Reactors Department, Atomic Energy Establishment, A.R. Egypt.

REFERENCES

1. V. S. Arpaci and J. A. Clark, Dynamic response of heat exchangers having internal heat sources, *J. Heat Transfer* **81C**, 253–266 (1959).
2. D. Feretic and M. M. Hilal, Transient heat transfer in a model of reactor channel, UAR Atomic Energy Establishment Report No. 16 (1965).
3. D. Feretic and M. A. Sultan, Frequency and spectral analysis of characteristic temperatures in reactor channel, *Atomkernenergie* **11**, 441–445 (1966).
4. J. F. Thorpe, Axial heat conduction in reactor fuel elements, *Nucl. Sci. Engng* **23**, 329–334 (1965).
5. K. O. Solberg and P. Bakstad, A model for the dynamics of nuclear reactors, Institut for Atomenergi, Kjeller, IR-121 (1967).
6. G. M. Zaki, Unsteady-state heat transfer in a reactor channel model, Unpublished M.Sc. Thesis, Faculty of Engineering, Cairo University (1970).
7. G. Doetsch, *Guide to the Applications of Laplace Transforms*, pp. 68–71. Van Nostrand, London (1961).
8. A. Abramowitz and I. A. Stegun, *Handbook of Mathematical Functions*, p. 379. Dover, New York (1965).
9. M. Jakob, *Heat Transfer*, Vol. 1, p. 552. Wiley, New York (1949).

CONVECTION A PARTIR D'UN TUBE AVEC UNE GENERATION HARMONIQUE DE CHALEUR

Résumé—On étudie, à la fois expérimentalement et théoriquement, le comportement dynamique des éléments de chauffage tubulaires avec génération interne harmonique de chaleur. L'analyse est basée sur la méthode de "réponse fréquentielle". Les résultats sont donnés en termes de critères pratiques pour l'ingéniérie. La technique expérimentale utilisée est rapidement décrite. Les résultats à laquelle elle conduit s'accordent avec ceux de l'analyse.

KONVEKTION AN EINEM ROHR MIT HARMONISCHER INNERER WÄRMEERZEUGUNG

Zusammenfassung—Das dynamische Verhalten von Rohrheizelementen bei harmonischer innerer Wärmeerzeugung wird experimentell und analytisch mit Hilfe der "Frequenz-Antwort-Methode" untersucht, und die Ergebnisse werden in Form der gebräuchlichen "Ingenieur"-Kriterien dargestellt. Es ist eine gute Übereinstimmung der gemessenen mit den errechneten Werten vorhanden. Die angewandte experimentelle Technik wird kurz beschrieben.

КОНВЕКЦИЯ ОТ ТРУБЫ ПРИ ГАРМОНИЧЕСКОМ ВНУТРЕННЕМ ГЕНЕРИРОВАНИИ ТЕПЛА

Аннотация — Аналитически и экспериментально исследуются динамические характеристики трубчатых нагревательных элементов при гармоническом внутрением генерировании тепла. Анализ проводится методом «частных характеристик». Полученные результаты представлены в виде обычных «инженерных» критериев. Кратко описывается используемый экспериментальный метод; полученные результаты хорошо согласуются с данными анализа.